

Exploration of a W/O Nanoemulsion for Antibiofilm Activity against Cariogenic *Enterococcus faecalis*

Manvi Singh,[∇] Abdul Rehman,[∇] Nazia Hassan, Abdul Anfey Faheem, Ayan Das, MohammadAkhlakuer Rahman, Mohammad Javed Ansari, Nilima Sharma, Mridu Dudeja, Mohd Aqil, Mohd. Aamir Mirza,* and Zeenat Iqbal*



Cite This: *ACS Omega* 2023, 8, 2871–2879



Read Online

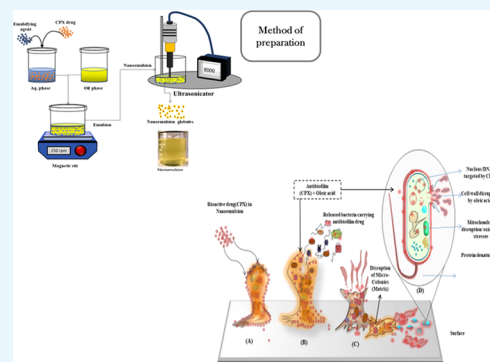
ACCESS |

Metrics & More

Article Recommendations

Supporting Information

ABSTRACT: A ciprofloxacin-loaded water-in-oil nanoemulsion (CPX-NE) was prepared and evaluated for the antimicrobial effect against oral biofilms produced by *Enterococcus faecalis*. CPX-NE was prepared by ultrasonication using functional excipients oleic acid (oil phase), Span 80 (surfactant), and Transcutol P (cosurfactant). Rheological parameters (viscosity = 20 ± 1.24 cp) confirmed optimum values for CPX-NE, a pH of 6.5 ± 0.23 suggested the simulation of CPX-NE with the pH of the mouth cavity, refractive index (1.46 ± 0.22), and % transmittance (92.34 ± 0.02) indicated the isotropic nature of the NE. The droplet size (72.19 ± 1.68 nm), polydispersity index (0.142 ± 0.02), and ζ potential (-28 mV) demonstrated a narrow size distribution and electrostatically stabilized NE. The morphology of the optimized formulation showed uniform spherical nanodroplets, as seen in fluorescence microscopy. In vitro drug release showed an initial burst effect followed by sustained release for 48 h, following Fick's diffusion. The minimum biofilm inhibitory and eradication concentration (MBIC/MBEC) was determined to compare CPX-NE with ciprofloxacin plain drug solution (CPX-PS) for their efficacy. CPX-NE demonstrated a significant inhibitory and eradication effect compared to CPX-PS. It was concluded that the developed CPX-NE has effective antibiofilm activity against *E. faecalis* and may be useful in the prevention and treatment of dental caries.



INTRODUCTION

Dental caries still affects people of all ages worldwide and is a global health concern despite all efforts to manage and prevent it. The most common infectious disease in the oral cavity is dental caries, sometimes known as tooth decay, which spreads by alternating demineralization and remineralization rather than unidirectional demineralization.¹ Microorganisms have a special ecological niche in the oral cavity, where they typically build up on tooth surfaces to produce dental plaque/oral biofilms. The principal causative agents of dental caries are cariogenic bacteria that may ferment carbohydrates to create acid and further demineralize the tooth surfaces.^{2–4} A wide variety of bacteria are involved in the production of dental biofilms.^{5,6} Among all, *Enterococcus faecalis* (*E. faecalis*) is a Gram-positive coccus and facultative anaerobe detected in resistant endodontic infections. This species survives under unfavorable environments with poor nutritional conditions. *E. faecalis* can penetrate the dentin tubules and form a biofilm, leading to an increase in microbial resistance and the failure of endodontic treatment.^{7,8} Therefore, preventing the development of plaque biofilms is essential for the effective management and prevention of dental caries. The mechanical clearance of oral biofilms continues to be the top option for the prevention of dental caries and periodontal disorders at the

moment. At the same time, the introduction of antibiotics has provided medical professionals with a fresh way to combat dental caries.⁹

The most effective antibacterial agent against oral biofilms at the moment is chlorhexidine. However, the use of chlorhexidine in oral care is restricted due to its potential for negative side effects such as tooth discoloration and its disagreeable taste. As a result, an effective formulation strategy was required to overcome the shortcomings of the current formulation and chlorhexidine. The formulations of antimicrobials in nanoforms and different vesicular systems have enhanced their efficacy and selective delivery to both extracellular and intracellular infections, as well as their antibiofilm activity, compared to the free drug.¹⁰ Nanoemulsions as drug delivery systems have several advantages such as the solubilization of hydrophobic compounds, excellent stability, commercial scalability, sustained release, reduction of toxicity, and

Received: May 22, 2022

Accepted: November 14, 2022

Published: January 11, 2023



promotion of drug activity.^{11,12} Nanoemulsions (NEs) mainly comprise of oil, surfactant, cosurfactant, and water, and their application as antimicrobial agents is a new and promising innovation.^{13,14} During their production, ultrasonication provides the necessary energy input for the droplet to break into nanodroplets and produce kinetically stable nanoemulsions.^{15,16} The research into the use of a nanoemulsion as an antimicrobial agent was encouraged by the recognized problem of the emergence of antimicrobial-resistant strains. The development of antimicrobial-resistant strains was experienced with the use of existing agents due to their prevalence and occasionally wrong use of antibiotics, disinfectants, and antiseptics.¹⁷ The need for new antimicrobial agents that target specific pathogens while being safe for the patient justifies additional research and development in light of these drawbacks. Nanoemulsions would not cause the development of resistant strains because their mode of action appears to be the nonspecific breakdown of bacterial cell membranes. It has been proposed that the molecular structure of a nanoemulsion adversely affects the integrity, form, and function of the bacterial cytoplasmic membrane, causing consequent internal damage to the cell.¹⁸ On the other hand, it has been shown that the nanoemulsion has broad biocidal efficacy against bacteria, enveloped viruses, and fungi by disrupting their outer membranes.^{19,20} Moreover, there are several published reports that nanoemulsions are effective against biofilms.^{21–23} An oil-in-water (o/w) nanoemulsion helps in solubilizing lipophilic drugs and protects the drugs from hydrolysis or oxidation as the drugs will be in the oily phase. However, a water-in-oil (w/o) nanoemulsion has an outer lipid layer and an inner aqueous layer. Water is necessary for bacterial growth and reproduction, but bacteria cannot survive in pure fat or oil. The importance of developing w/o nanoemulsions is that they have significant antimembrane activity, which results in the dysfunction and disturbance of the cytoplasmic membrane structure, causing consequent internal damage to the cell.¹⁸ Therefore, the use of nanoemulsions to control the adhesion and biofilm formation of cariogenic bacteria on the tooth surface is a logical approach to prevent this common oral disease. Ciprofloxacin hydrochloride (CPX) is one of the common drugs used for endodontic infections. The effective action against oral anaerobes, Gram-positive aerobic organisms (*Staphylococcus aureus*, *Enterobacter* species, and *Pseudomonas*), demands the need of CPX for endodontic infections, which is supposed to be on the verge of resistance. Our research aims to develop a w/o nanoemulsion containing CPX for localized and targeted drug delivery for biofilm disruption.

RESULTS

Selection of Suitable Excipients. To achieve optimum drug loading, solubility studies for the drug were carried out in different oils, surfactants, and cosurfactants (Table 1). For the selection of oil, a maximum solubility of $6.9 \pm 0.4 \mu\text{g/mL}$ was observed in oleic acid. The maximum solubility of CPX was found in Span 80 as a surfactant and Transcutol P as a cosurfactant. The commercial success of any formulation relies on its regulatory compliance, and therefore, the excipients used to prepare the purported formulation were selected cautiously. Table 2 summarizes the regulatory status of the excipients used.

Pseudoternary Phase Diagram. Different S_{mix} ratios were taken, as shown in Table 3, and slowly titrated with oleic

Table 1. Solubility of CPX in Different Excipients (Oils, Surfactants, and Cosurfactants)

Name of excipient	Solubility ($\mu\text{g/mL}$)
coconut oil	5.6 ± 0.14
oleic acid	6.9 ± 0.23
olive oil	4.9 ± 0.36
Span 80	2350 ± 0.23
Transcutol HP	1050 ± 0.56
Peceol	654 ± 0.18
Cremophor EL	570 ± 0.48
PEG 400	890 ± 0.08
Transcutol P	1800 ± 0.89
propylene glycol	980 ± 0.99
ethanol	697 ± 0.38

acid till transparent, cloudy, or turbid systems were obtained. The points at which a clear transparent homogeneous nanoemulsion was formed were noted and plotted using PCP-triangular software. Two phase diagrams were obtained with 2:1 and 1:1 weight ratios of Span 80 and Transcutol P, respectively (Figure 1). A pseudo-three-component phase diagram was constructed with the first axis showing the aqueous phase, the second axis showing the oily phase, and the third axis representing the mixture of the surfactant and the cosurfactant at a fixed mass ratio. The highlighted area depicts the formation of the nanoemulsion region. An S_{mix} ratio of 1:1 showed a lesser region for nanoemulsion formation when compared with an S_{mix} ratio of 2:1. Therefore, the S_{mix} ratio of 2:1 was chosen for the nanoemulsion formation.

Ciprofloxacin-Loaded Nanoemulsion Formulation. A CPX-loaded nanoemulsion was prepared by the method described above. Briefly, CPX (16 mg/ml) was dissolved in the optimized mixture of 45% w/w S_{mix} of Span 80 (30% w/w) and Transcutol P (15% w/w) and slowly oleic acid was added to the mixture with continuous vortexing to produce a clear nanoemulsion. Further, the clear nanoemulsion was ultrasonicated at 20 kHz for 5 s.

Thermodynamic Stability Studies. The formulations were subjected to cycles of heating and cooling, freeze–thawing, and centrifugation. The formulation (F5) proved to be stable and isotropic, as it showed no phase separation, cracking, creaming, coalescence, or phase inversion, as shown in Table 4.

Rheological Parameters. Table 5 shows the various rheological parameters for the selected formulations (F1, F2, and F5) after thermodynamic stability studies. The viscosity of the optimized formulation (F5, designated as CPX-NE) was found to be 20 ± 1.24 cp. The pH of F5 was measured to be 6.5 ± 0.23 , which is in accordance with the pH (6.4–6.8) of the mouth cavity.²⁴ The refractive index and % transmittance were found to be 1.46 ± 0.22 and $92.34 \pm 0.02\%$, respectively, indicating the isotropic nature of the nanoemulsion. A value of percentage transmittance closer to 100% indicates that the optimized formulation is clear and transparent.

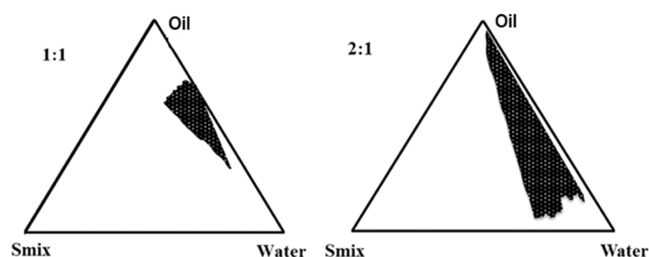
Nanoemulsion Characterization. The photon correlation spectroscopy was used to determine the droplet size of the nanoemulsion and the size distribution. Droplet size and PDI are important factors that describe the uniformity, quality, dispersibility, and stability of nanoemulsions. The particle size of the nanoemulsion before sonication was found to be 249.3 ± 1.94 nm with a PDI of 0.234 ± 0.08 . The droplet size was reduced to 72.19 ± 1.68 nm with a PDI of 0.142 ± 0.02 after

Table 2. Regulatory Requirements for Functional Excipients

Common name	Oleic acid	Transcutol P	Span 80
USP NF name	9-octadecenoic acid	diethylene glycol monoethyl ether	sorbitan ester
EP name	<i>cis</i> -9-octadecenoic acid, elainic acid	diethylene glycol monoethyl ether	sorbitan monooleate
CAS no.	112-80-1	111-90-0	1338-43-8
maximum potency per unit dose (as per IIG database)	0.03% w/v	49.9% w/w	150 mg/ml
relevant physiochemical properties	viscosity, 27.64 mPa/s ⁻¹ at 25 °C HLB value, 1	viscosity, 4.8 mPa/s ⁻¹ at 20 °C HLB value, 4.2	viscosity, 1000–4000 mPa/s ⁻¹ at °C HLB value, 4.3
GRAS listed	√	√	√

Table 3. Visual Observation for Nanoemulsion Formulation

S _{mix} (Span 80: Transcutol P)	Formulation	Water:S _{mix}	Inference
1:1	F1	1:9	nanoemulsion
	F2	1:8	nanoemulsion
	F3	1:7	turbid
1:2	F4	1:9	turbid
	2:1	F5	1:9
F6		1:8	cloudy
F7		1:7	cloudy
F8		1:6	turbid
F9		1:5	turbid

**Figure 1.** Pseudo-three-component phase diagram with S_{mix} ratios of 1:1 and 2:1.**Table 4. Thermodynamic Stability Studies of Selected Formulation from Ternary Phase Diagram**

S _{mix}	Water:S _{mix}	Formulation	Centrifugation	Heating-Cooling	Freeze-thaw cycle
1:1	1:9	F1	√	×	×
1:1	1:8	F2	×	×	√
2:1	1:9	F5	√	√	√

(√) Phase separation, (x) no phase separation.

sonication for 5 s at 20 kHz (Figure 2a). The smaller size of the nanoemulsion ensures better permeation due to enhanced surface area. The lesser the PDI, the more the uniformity of the droplets in the formulation.

For electrostatically stabilized nanoemulsions, the ζ potential value should be in the range of ± 30 mV.²⁵ The ζ potential value obtained was −28.0 mV, which was indicative of an electrostatically stabilized nanoemulsion. The shape and uniformity of the nanodroplets in the optimized formulation

were determined by fluorescence microscopy. Experimentally, the morphology of the optimized formulation showed uniform spherical nanodroplets, as shown in Figure 2b. The drug content in the optimized formulation was found to be 98.7 ± 0.67%, which showed the good drug loading capacity of the nanoemulsion, which is an essential requirement for the nanoemulsion.

In Vitro Drug Release Study. The drug release behavior of optimized formulation F5 in phosphate-buffered saline (PBS, pH 5.5) and artificial saliva (pH 6.8) was observed and compared with the plain solution of the drug (CPX-PS) using the dialysis membrane method (Figure 3a). CPX-NE showed a cumulative release of 78.9% compared to the 40.5% release of CPX-PS in 48 h in PBS, pH 5.5 buffer. On the other hand, CPX-NE showed a cumulative release of 82.1% compared to the 42.3% release of CPX-PS in artificial saliva pH 6.8 at the same time (Figure 3b).

Drug Release Kinetics. The release data were fitted into various release kinetics models, and linear regression analysis was done (Supporting Figure 1). The best-fitting model was the first-order release followed by Korsmeyer–Peppas kinetics with regression coefficients (R²) of 0.842 and 0.904, respectively. The *n* value of 0.09 suggested that CPX-NE followed Fickian diffusion release behavior.

Antibiofilm Activity. Minimum Biofilm Inhibitory and Eradication Concentration. *E. faecalis* biofilm was formed and tested for the efficacy of CPX-NE. Figure 4 shows the antibiofilm activity of CPX-NE compared with CPX-PS. CPX-NE inhibited the biofilm at a concentration of 16 μg/mL compared with CPX-PS, which inhibited the biofilm at a concentration of 256 μg/mL. On the other hand, the MBEC observed for CPX-NE and CPX-PS were found to be 64 and 1024 μg/mL, respectively. Results suggested that both inhibitory and eradication concentrations of CPX-NE were 16-fold smaller than those of CPX-PS.

Visualization of the Biofilm. Fluorescence microscopy was used to visualize the presence of the *E. faecalis* biofilm formed on the ELISA plate. The photomicrograph was taken 48 h after the biofilm was treated with CPX-NE. Figure 5i shows the *E. faecalis* biofilm before the treatment with CPX-NE. Figure 5ii shows the inhibition or eradication of the *E. faecalis* biofilm after treatment with CPX-NE.

Stability Study. The droplet size, PDI, and pH of the nanoemulsion were measured during the stability study, and

Table 5. Rheological Parameters of Selected Formulation after the Thermodynamic Stability Test

Formulation	Viscosity (cp)	pH	Refractive index	(%) Transmittance
F1	14 ± 0.21	6.2 ± 0.34	1.43 ± 0.12	95.45 ± 0.08
F2	16.21 ± 0.88	6.4 ± 0.15	1.44 ± 0.19	94.21 ± 0.06
F5	20 ± 1.24	6.5 ± 0.23	1.46 ± 0.22	92.34 ± 0.02

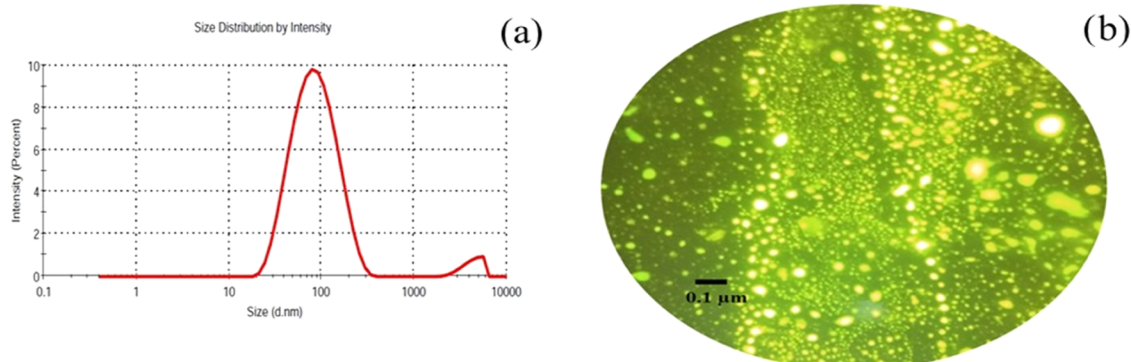


Figure 2. (a) Particle size of the optimized formulation. (b) Fluorescence microscopy of the optimized formulation.

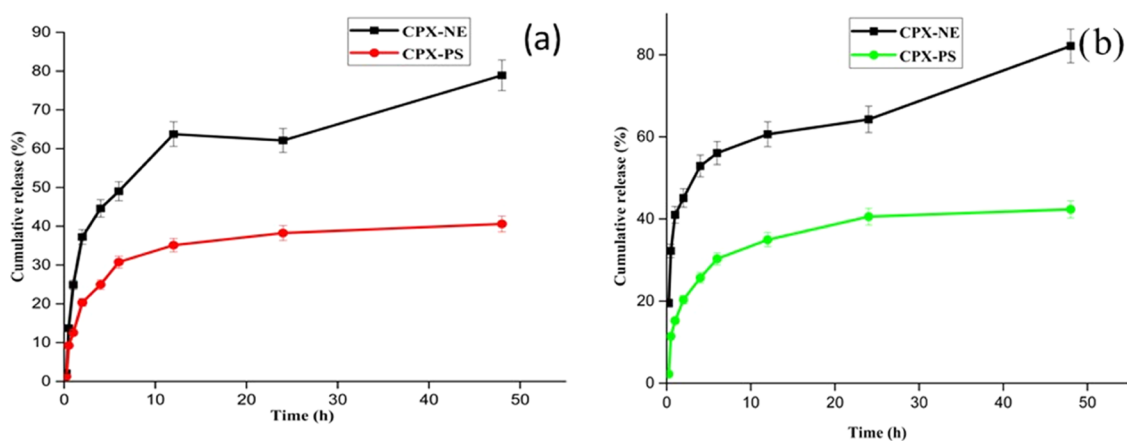


Figure 3. (a) In vitro release of CPX-NE in PBS buffer pH 5.5. (b) In vitro release of CPX-NE in artificial saliva pH 6.8.

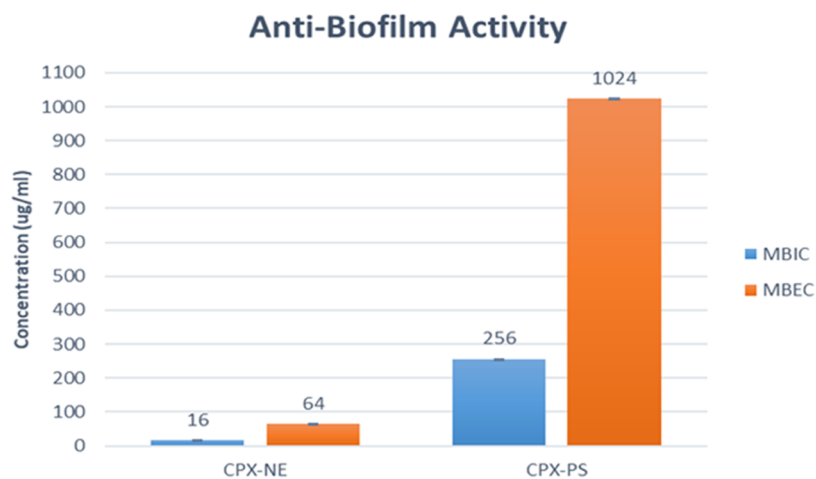


Figure 4. Antibiofilm activity of CPX-NE and CPX-PS.

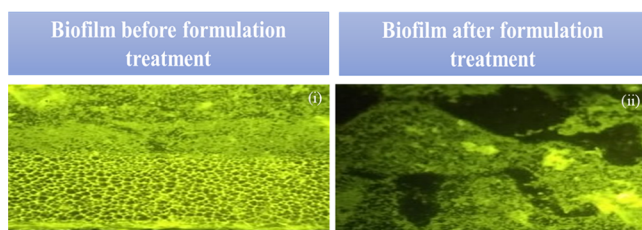


Figure 5. Visualization of biofilm formation (i) before and (ii) after treatment with CPX-NE.

the results are shown in Table 6. The nanoemulsion had an initial mean diameter of 72.19 ± 1.68 nm and maintained the size at 74.52 ± 1.82 and 77.45 ± 1.23 nm for 180 days under refrigeration ($8\text{ }^{\circ}\text{C}$) and at room temperature ($25\text{ }^{\circ}\text{C}$), respectively. The PDI value of the nanoemulsion was kept below 0.2 at temperatures of 8 and $25\text{ }^{\circ}\text{C}$ during the stability study. However, a decrease in the pH of the nanoemulsion stored at room temperature and in the refrigerator was observed during the stability study.

Table 6. Stability Study of the Nanoemulsion Stored in the Refrigerator (8 °C) and at Room Temperature (25 °C)^a

Storage temp. (°C)	Day	Droplet size (nm) ± SD	PDI ± SD	pH ± 0.23
8	0	72.19 ± 1.68	0.142 ± 0.02	6.5 ± 0.23
	15	72.78 ± 1.34	0.147 ± 0.05	6.5 ± 0.16
	30	72.96 ± 1.27	0.155 ± 0.02	6.4 ± 0.13
	60	73.45 ± 1.09	0.163 ± 0.05	6.6 ± 0.09
	90	74.06 ± 1.16	0.176 ± 0.04	6.4 ± 0.14
25	180	74.52 ± 1.43	0.182 ± 0.01	6.3 ± 0.20
	0	72.19 ± 1.68	0.142 ± 0.02	6.5 ± 0.23
	15	72.96 ± 1.25	0.153 ± 0.05	6.6 ± 0.18
	30	73.65 ± 1.83	0.159 ± 0.02	6.5 ± 0.11
	60	75.27 ± 1.17	0.163 ± 0.04	6.4 ± 0.16
25	90	76.13 ± 1.29	0.179 ± 0.05	6.3 ± 0.21
	180	77.45 ± 1.23	0.195 ± 0.06	6.2 ± 0.15

^aSD = standard deviation. Results are mean ± SD ($n = 3$).

DISCUSSION

A water-in-oil nanoemulsion is prepared using oil, surfactant, and cosurfactant. Oleic acid was selected as the oil phase for the w/o nanoemulsion due to its property of repressing the biofilm formation by blocking bacterial adhesion to the surface.²⁶ It has been expected that addition of oleic acid will have a synergistic effect in inhibiting the biofilm formation. It would act as a functional excipient and additionally skill up the prepared nanoemulsion. Span 80 was selected due to the presence of long saturated alkyl chains, which act as a contributing factor in the permeability of the nanoemulsion. The long saturated alkyl chain of Span 80 helps to prepare nanoemulsion formulations that are less leaky and retain the encapsulated drug.²⁷ Also, the surfactant and cosurfactant were selected based on the hydrophilic and lipophilic balance of Span 80 (HLB = 4.3) and Transcutol P (HLB = 4.2), suggesting its suitability for the w/o nanoemulsion. The pseudoternary phase diagram helps in the selection of the S_{mix} ratio, as a low amount of S_{mix} helps to minimize the interfacial tension. Thus, increasing the interfacial area and thus lowering the system's free energy to a meager value result in a spontaneous dispersion that is a thermodynamically stable nanoemulsion. The difference between nanoemulsions and microemulsions is that nanoemulsions are kinetically stable, hence phase separation cannot be seen.²⁸ Hence, for physically and thermodynamically stable nanoemulsions, accurate concentrations of water, oil, surfactant, and cosurfactant should be used. Viscosity is a major factor in determining the resistance for the flow of fluid in nanoemulsions. It is basically dependent on the molecular volume and the number of carbon atoms. In the current study, oleic acid being the oily phase structurally contains C-18 unsaturated fatty acid in addition to Span 80 and Transcutol P that contributes to increasing the viscosity of the nanoemulsion. The smaller the particle size, the more the efficacy of the formulation to eradicate biofilms with the least concern about antibiotic resistance.²⁹ PDI helps in determining the size distribution and nature of the dispersion of the formulation. PDI in the range of ≤ 0.5 indicates a narrow size distribution and the highest quality of dispersion; therefore, smaller PDI will show homo-distribution of nanoemulsion droplets.³⁰ The ζ potential's negative value is due to the presence of an anionic group present in the fatty acid of oil and surfactant. The implication of ζ potential is related to the

stability of the formulation, controls interactions between the charges on the particles, and shows the degree of repulsion among the similarly charged particles in a solution.³¹ Repulsive forces will help in preventing flocculation and aggregation of the nanoemulsion droplets. The initial burst release can be attributed to the fact that the small size of the nanoemulsion droplet provides a larger surface area for the drug to release. Thereby, a faster rate of drug release can be observed, as approx. 60% of CPX was released in 12 h with sustained release afterward for a period of 48 h. Hydrophilic drugs incorporated into the nanoemulsion follow first-order release kinetics. This model showed that the rate of drug release was proportional to the concentration of the drug in the formulation, and it decreased with time.³² The mechanism of the drug release pattern was established by the Korsmeyer–Peppas model by calculating the n value from the slope of the curve, which showed that the drug was released from a region of higher concentration to a region of lower concentration.³³ Biofilm construction by microbes like *E. faecalis* in the oral cavity has made periodontal therapy quite challenging. A nanoemulsion containing CPX and oleic acid was prepared successfully by the ultrasonication technique. The values of MBIC and MBEC compared to the plain drug solution (CPX-PS) showed that CPX-NE could be used as an antibiofilm product. Oral microbial flora that adheres to, detaches from, and accumulates on the tooth surface controls the development of dental biofilms. Therefore, the initial steps of adhesion and colonization are critical for the creation of biofilms. Typically, the exposure of the nanoemulsion for 48 h led to the maximum reductions in biofilms and significantly decreased the number of planktonic forms. Fluorescent microscopy clearly showed that *E. faecalis* was disrupted after treatment with the optimized formulation. In summary, the purported CPX-NE could emerge as an excellent tool to disrupt the biofilm and prevent its adherence to the tooth surface while arresting the progression of the *E. faecalis*-induced periodontal infection. Also, a regulatory perspective in selecting the nanoemulsion components would further substantiate its commercial viability.

During the stability study, increases in the mean diameter of the nanoemulsion droplets and PDI stored at room temperature and under refrigeration were detected. However, the statistical analysis showed that the increases were not statistically significant ($p < 0.05$). PDI values below 0.3 are near to monomodal size distribution.¹² However, decreases in the pH of the nanoemulsion stored at room temperature and in the refrigerator were observed during the stability study. Meanwhile, the statistical analysis showed that the decreases were not statistically significant ($p < 0.05$). The formulation was clear and transparent in appearance after 6 months of the study period.

MATERIALS AND METHODS

Materials. Ciprofloxacin was provided as a gift sample by Wings Biotech, Baddi, Himachal Pradesh, India. Oleic acid was obtained from Gattefosse Corp. (India). Span 80 and Transcutol P were purchased from Merck (India). All other chemicals used in the study were of analytical reagent grade.

Methods. Screening of Nanoemulsion Components. The solubility of CPX was determined in different nanoemulsion components, namely, oils (oleic acid, olive oil, coconut oil), surfactants (Span 80, Transcutol HP, Peceol, Cremophor EL, PEG 400), and cosurfactants (Transcutol P, ethanol, propylene

glycol). Briefly, an excess amount of drug was added to 2 mL of each excipient separately in 5 mL capacity of stoppered glass vials. These vials were first vortexed for 5 min using a vortex mixer and then kept at 37 °C in an isothermal shaker (Nirmal International, Delhi, India) for 72 h to achieve equilibrium. The equilibrated samples were then centrifuged at 3000 rpm for 15 min using a centrifuge (Remi, India). The supernatant was then filtered using a 0.45 μm membrane filter. Finally, the CPX concentration in selected excipients was analyzed by a UV spectrophotometer at 280 nm.³⁴

Pseudoternary Phase Diagram Construction. For the construction of the pseudoternary phase diagram, the components of the nanoemulsion were selected based on the solubility studies of CPX in oils, surfactants, and cosurfactants. The pseudoternary phase diagrams consisting of oil, S_{mix} (surfactant to cosurfactant ratio), and distilled water were developed.³⁵ The surfactant and cosurfactant (S_{mix}) in different weight ratios (1:1, 1:2, 1:3, 1:4, 2:1, 3:1, 4:1) were prepared with increasing surfactant concentration with respect to the cosurfactant and the increasing concentration of the cosurfactant with respect to the surfactant. Sixteen different combinations of water and S_{mix} : 1:9, 1:8, 1:7, 1:6, 1:5, 2:8, 1:3.5, 1:3, 3:7, 1:2, 4:6, 5:5, 6:4, 7:3, 8:2, 9:1, were prepared and titrated with oil slowly till a clear transparent liquid was obtained. Different combinations in different weight ratios of S_{mix} and water were used so that maximum ratios remained covered to outline the phase boundaries in the phase diagrams. The pseudoternary phase diagrams were constructed using PCP-Triangular software. The visual observations were recorded for the formation of a gel, milky white, or transparent nanoemulsion (Table 1).

Preparation of the Ciprofloxacin Nanoemulsion. Different combinations of nanoemulsion formulations were chosen from each of the phase diagrams constructed from the nanoemulsion region for drug incorporation into the aqueous phase; 16 mg/mL CPX was dissolved in an aqueous phase (distilled water) for all selected nanoemulsion formulations. Then, the preset quantity of S_{mix} (Span 80 and Transcutol P) was added to the aqueous solution of the drug and stirred for 2 min. The oil phase (oleic acid) was added slowly with continuous stirring. Further, the clear w/o nanoemulsion was subjected to ultrasonication for a time period of 5, 10, and 15 s at 20–40 kHz.³⁶

Thermodynamic Stability Test. Thermodynamic stability testing was carried out to avoid the formation of a metastable formulation.²⁸ The formulation was centrifuged at 3000 rpm for 20 min followed by three cycles of heating and cooling interchangeably at 4 and 45 °C for 24 h. Finally, the freeze-thaw cycle was carried out by storing the formulation at –21 °C for 24 h and then at +21 °C. The nanoemulsion was visually inspected for any sign of instability.

Determination of Rheological Parameters. Viscosity. The viscosity of the nanoemulsion was determined without dilution using a Brookfield R/S plus rheometer (Brookfield Engineering Laboratories, Inc., Middleboro, MA) using a spindle CPE40 at 25 °C. The software used was Rheocalc V2.6.

Clarity. The consistency of the formulation was evaluated using a clarity test by measuring the percentage (%) transmittance at 630 nm against water as blank. For this purpose, 2 mL of the nanoemulsion was placed in a cuvette, and % transmittance was recorded.

Refractive Index. The refractive index of the nanoemulsion was measured using an Abbe refractometer (Bellingham & Stanley Refractometer, RFM840 Type 26–840).

pH. The pH of the nanoemulsion was measured using a pH meter (Mettler Toledo MP 220, Greifensee, Switzerland) at 25 °C.

Nanoemulsion Characterization. Particle Size and Polydispersity Index (PDI). Droplet size and size distribution were determined using photon correlation spectroscopy based on laser light scattering phenomena. Two milliliters of the nanoemulsion was taken in a cuvette and scanned using a Zetasizer 1000 HAS (Malvern Instrument, U.K.). The scattering of the light was monitored at 25 °C at a 90° angle.³⁷

Particle Charge/ ζ Potential. The particle charge is quantified as the ζ potential value, measured via the electrophoretic mobility of particles in an electrical field. The ζ potential of the optimized formulation was measured using a Zetasizer 1000 HAS (Malvern Instrument, U.K.).

Fluorescence Microscopy. The morphology of the nanoemulsion was determined by fluorescence microscopy. Briefly, 2 mL of the nanoemulsion was labeled with rhodamine dye and left for 10 min. Further, the slides were prepared with the complex containing rhodamine and the nanoemulsion was submitted for evaluation by a fluorescence microscope for imaging.

Drug Content. Methanol tends to dissolve and break the components of a nanoemulsion. The drug content was calculated by dissolving the nanoemulsion in methanol. The sample was then centrifuged at 3000 rpm for 15 min, and then the supernatant was collected, filtered, and analyzed for drug content using a UV spectrophotometer at 280 nm.

In Vitro Drug Release Study. The study was carried out using a dialysis membrane (MW cut off 12,000 gm/mol; Sigma). Before using the dialysis bag, it was rinsed with running water for 3–4 h to remove glycerin, followed by treatment with a 0.3% w/v sodium sulfide solution for 1 min to remove the sulfur components and then further washed with hot water for 2 min. Further, the membrane was treated again with 0.2% v/v sulfuric acid to remove the acid and then stored in dissolution media at 2–8 °C until used. Then, 1 mL of the nanoemulsion was loaded in dialysis bags (equivalent to 16 mg of CPX) and immersed in 100 mL of phosphate buffer pH 5.5, 37 ± 0.5 °C at 100 rpm for 48 h.³⁸ The dissolution study was also carried out in 200 mL of the preformed artificial saliva pH 6.8, 37 ± 0.5 °C at 100 rpm for 48 h. The samples were withdrawn, and the drug content was analyzed using a UV spectrophotometer at 280 nm. A graph was plotted between % drug release and time for plain CPX solution (CPX-PS) and the optimized formulation (CPX-NE).

Drug Release Kinetics and Mechanism. For the analysis of the drug release mechanism from the nanoemulsion delivery system, the data were subjected to kinetic evaluation using various models such as zero-order, first-order, Higuchi, Korsmeyer–Peppas, and Hixon Crowell models using an excel add-in program DDSolver. The mechanism of drug release was studied using the Peppas equation given below

$$\frac{M_t}{M_\infty} = K_m t^n$$

where M_t is the cumulative amount of drug released at time t , M_∞ is the amount released at infinite time, K_m is a constant characteristic of the drug–polymer system, and n is the

diffusion exponent indicating the nature of the release mechanism.

Antibiofilm Activity. Biofilm Formation. Biofilm formation was achieved by a previously described method.³⁹ Briefly, for each strain, one colony was transferred to tryptic soy broth (TSB) and incubated overnight under stationary aerobic conditions at 37 °C. The cultures were diluted (1:100) in medium, and 200 μ L of this cell suspension was dispensed into sterile flat-bottom 96-well polystyrene microtiter plates. For every strain, four wells were inoculated. TSB alone was dispensed into eight wells as a negative control. After incubation, the broth was carefully drawn off by a multichannel pipettor. The wells were washed three times with 200 μ L of phosphate-buffered saline. The biofilms were fixed with 200 μ L of Bouin's Fixative for 30 min, and the wells were washed with distilled water. The biofilms were stained with 200 μ L of 1% crystal violet solution in water for 30 min, and the wells were washed with distilled water. The microtiter plates were inverted on a paper towel and air-dried.

Determination of Minimum Biofilm Inhibitory Concentration (MBIC). The antibiofilm activity of CPX-NE was compared with that of CPX-PS, through determination of MBIC. Biofilms were allowed to form in the presence of different concentrations of CPX-PS and CPX-NE (8–512 μ g/mL). The MBIC was determined as the lowest concentration of the formulation with the mean biofilm optical density (OD) less than or equal to the optical density of the negative control measured at 570 nm. Uninoculated Tryptic Soy broth was used as a negative control, while plain *E. faecalis* culture was used as a positive control.²⁷

Determination of Minimum Biofilm Eradication Concentration (MBEC). MBEC evaluates the ability of the formulation to eradicate the already-formed biofilms. The tested strains were allowed to form biofilms. Wells were then washed with sterile distilled water, and 200 μ L of each formulation (8–512 μ g/mL) of CPX-PS and CPX-NE was added. Plates were incubated for 24 h aerobically at 37 °C, and the OD of biofilms was measured at 570 nm. Uninoculated TSB was used as a negative control, while plain *E. faecalis* culture was used as a positive control. The MBEC was determined as the lowest concentration giving the mean biofilm OD less than or equal to the OD of the negative control.²⁷

Visualization of Biofilm Fluorescent Microscopy. Biofilm formation by *E. faecalis* was visualized by a fluorescence microscope after staining it with Calcofluor white for 15 min in the dark. Extracellular polymeric substances (EPS) of *E. faecalis* were observed through a Nikon Eclipse DAPI filter (excitation filter, 340 \pm 380 nm; dichroic mirror, 400 nm; barrier filter, 435 \pm 485 nm).

Stability Study. The droplet size, PDI, and pH of the optimized nanoemulsion formulation were investigated at 0, 15, 30, 60, 90, and 180 days of storage in the refrigerator (8 °C) and at room temperature (25 °C). The studies were performed in triplicate for each storage condition.

Statistical Analysis. All of the data are represented as mean \pm SD. One-way ANOVA was performed on all of the studies to determine the level of significance.

CONCLUSIONS

Nanoemulsions have emerged as one of the most versatile drug delivery tools due to their small size, optical transparency, tunable rheology, and robust stability without any flocculation for long-term storage. Ciprofloxacin HCl nanoemulsion (CPX-

NE) formulation was chosen as a tool to inhibit the *E. faecalis* biofilm with the intention of salvaging the dipping effect of CPX on *Enterococci*. A water-in-oil (w/o) nanoemulsion was fabricated with the high shear method of ultrasonication using oleic acid, Span 80, and Transcutol P. Thermodynamic and rheological parameters indicated the formation of the w/o nanoemulsion. Pseudoternary phase diagrams were constructed and the formulation was optimized with small size and uniform distribution. In vitro drug release was carried out in phosphate buffer and artificial saliva which showed Korsmeyer–Peppas model as the release mechanism having Fickian diffusion behavior. MBIC and MBEC of CPX-NE were found to be 16 times smaller than those of CPX-PS. Fluorescence images showed the inhibition or eradication of the *E. faecalis* biofilm before and after the treatment with CPX-NE. Thus, the w/o nanoemulsion can be used as a tool for biofilm eradication.

ASSOCIATED CONTENT

Supporting Information

The Supporting Information is available free of charge at <https://pubs.acs.org/doi/10.1021/acsomega.2c03180>.

(PDF)

AUTHOR INFORMATION

Corresponding Authors

Mohd. Aamir Mirza – Department of Pharmaceutics, School of Pharmaceutical Education and Research (SPER), Jamia Hamdard, New Delhi 110062, India; orcid.org/0000-0002-5780-7601; Email: aamir_pharma@yahoo.com

Zeenat Iqbal – Department of Pharmaceutics, School of Pharmaceutical Education and Research (SPER), Jamia Hamdard, New Delhi 110062, India; orcid.org/0000-0003-2788-9420; Email: zeenatiqbal@jamiahamdard.ac.in

Authors

Manvi Singh – Department of Pharmaceutics, School of Pharmaceutical Education and Research (SPER), Jamia Hamdard, New Delhi 110062, India; Department of Pharmaceutics, SGT College of Pharmacy, SGT University, Gurugram 122505, India

Abdul Rehman – Department of Pharmaceutics, School of Pharmaceutical Education and Research (SPER), Jamia Hamdard, New Delhi 110062, India

Nazia Hassan – Department of Pharmaceutics, School of Pharmaceutical Education and Research (SPER), Jamia Hamdard, New Delhi 110062, India

Abdul Anfeq Faheem – Department of Pharmaceutics, School of Pharmaceutical Education and Research (SPER), Jamia Hamdard, New Delhi 110062, India

Ayan Das – Department of Microbiology, Hamdard Institute of Medical Science and Research (HIMSR), Jamia Hamdard, New Delhi 110062, India

Mohammad Akhlaquer Rahman – Department of Pharmaceutics and Industrial Pharmacy, College of Pharmacy, Taif University, Taif 21944, Kingdom of Saudi Arabia

Mohammad Javed Ansari – Department of Pharmaceutics, College of Pharmacy, Prince Sattam Bin Abdulaziz University, Al-Kharj 16273, Saudi Arabia; orcid.org/0000-0001-9266-7133

Nilima Sharma – Department of Dentistry, HIMS & Hakim Abdul Hamid (HAH) Centenary Hospital, Jamia Hamdard, New Delhi 110062, India

Mridu Dudeja – Department of Microbiology, Hamdard Institute of Medical Science and Research (HIMSAR), Jamia Hamdard, New Delhi 110062, India

Mohd Aqil – Department of Pharmaceutics, School of Pharmaceutical Education and Research (SPER), Jamia Hamdard, New Delhi 110062, India

Complete contact information is available at:

<https://pubs.acs.org/10.1021/acsomega.2c03180>

Author Contributions

[▽]M.S. and A.R. contributed equally to this work. Dr. Z.I. and Dr. M.A.M. conceptualized the research idea, helped with data analysis, and reviewed the manuscript. M.S. and A.R. contributed to experimentation and writing of the original draft of the manuscript. M.S. also acquired funding for the project from the Indian Council of Medical Research (ICMR). Dr. A.D. contributed to the microbiological studies and data analysis. Dr. N.S. as a dentist helped in providing the periodontal patient sample having *Enterococcus faecalis*. Dr. M.A.R., M.A., Dr. M.J.A., and Prof (Dr.) M.D. contributed to the review and editing of the manuscript and shared their valuable inputs in improving the language and technicalities of the manuscript.

Notes

The authors declare no competing financial interest.

ACKNOWLEDGMENTS

M.S. is also thankful to the Indian Council of Medical Research (ICMR) for the SRF grant (45/62/2018-NAN-BMS), New Delhi, Government of India, for their financial support. Dr. M.J.A. acknowledges the support provided by the deanship of scientific research, Prince Sattam bin Abdulaziz University, Saudi Arabia.

REFERENCES

- (1) Hemingway, C. A.; Shellis, R. P.; Parker, D. M.; Addy, M.; Barbour, M. E. Inhibition of hydroxyapatite dissolution by ovalbumin as a function of pH, calcium concentration, protein concentration and acid type. *Caries Res.* **2008**, *42*, 348–353.
- (2) Beighton, D. Can the ecology of the dental biofilm be beneficially altered? *Adv. Dent. Res.* **2009**, *21*, 69–73.
- (3) Chandrabhan, D.; Hemlata, R.; Renu, B.; Pradeep, V. Isolation of dental caries bacteria from dental plaque and effect of tooth pastes on acidogenic bacteria. *Open J. Med. Microbiol.* **2012**, *02*, 65–69.
- (4) Lippert, F. The effects of lesion baseline characteristics and different Sr: Ca ratios in plaque fluid-like solutions on caries lesion de- and remineralization. *Arch. Oral Biol.* **2012**, *57*, 1299–1306.
- (5) Steinberg, D. *Studying Plaque Biofilms on Various Dental Surfaces Handbook of Bacterial Adhesion*; Springer, 2000; pp 353–370.
- (6) Marsh, P. D. Are dental diseases examples of ecological catastrophes? *Microbiology* **2003**, *149*, 279–294.
- (7) Afkhami, F.; Akbari, S.; Chiniforush, N. Enterococcus faecalis elimination in rootcanals using silver nanoparticles, photodynamic therapy, diode laser, or laser-activated nanoparticles: an in vitro study. *J. Endod.* **2017**, *43*, 279–282.
- (8) Miranda, R. G.; Santos, E. B.; Souto, R. M.; Gusman, H.; Colombo, A. P. V. Ex-vivo antimicrobialefficacy of the EndoVac system plus photodynamic therapy associated with calcium hydroxide against intracanal enterococcus faecalis. *Int. Endod. J.* **2013**, *46*, 499–505.

(9) Lima, G. Q. T.; Oliveira, E. G.; Souza, J. I. L. d.; Monteiro Neto, V. Comparison of the efficacy of chemomechanical and mechanical methods of caries removal in the reduction of *Streptococcus mutans* and *Lactobacillus* spp in carious dentine of primary teeth. *J. Appl. Oral Sci.* **2005**, *13*, 399–405.

(10) Wiater, A.; Choma, A.; Szczodrak, J. Insoluble glucans synthesized by cariogenic *Streptococci*: a structural study. *J. Basic Microbiol.* **1999**, *39*, 265–73.

(11) de Oliveira de Siqueira, L. B.; da Silva Cardoso, V.; Rodrigues, I. A.; Vazquez-Villa, A. L.; Dos Santos, E. P.; da Costa Leal Ribeiro Guimarães, B.; Dos Santos Cerqueira Coutinho, C.; Vermelho, A. B.; Junior, E. R. Development and evaluation of zinc phthalocyanine nanoemulsions for use in photodynamic therapy for *Leishmania* spp. *Nanotechnology* **2017**, *28*, No. 065101.

(12) Betzler de Oliveira de Siqueira, L.; Matos, A. P. D. S.; Cardoso, V. D. S.; Villanova, J. C. O.; Guimaraes, B. D. C. L. R.; Dos Santos, E. P.; Beatriz Vermelho, A.; Santos-Oliveira, R.; Ricci Junior, E. Clove oil nanoemulsion showed potent inhibitory effect against *Candida* spp. *Nanotechnology* **2019**, *30*, No. 425101.

(13) Tenjarla, S. Microemulsions: an overview and pharmaceutical applications. *Crit. Rev. Ther. Drug Carrier Syst.* **1999**, *16*, 461–521.

(14) Sonnevile-Aubrun, O.; Simonnet, J. T.; L'Alloret, F. Nanoemulsions: a new vehicle for skincare products. *Adv. Colloid Interface Sci.* **2004**, *108–109*, 145–9.

(15) Kumar, M.; Bishnoi, R. S.; Shukla, A. K.; Jain, C. P. Techniques for formulation of nanoemulsion drug delivery system: a review. *Prev. Nutr. Food Sci.* **2019**, *24*, 225–234.

(16) Setya, S.; Talegaonkar, S.; Razdan, B. Nanoemulsions: formulation methods and stability aspects. *World J. Pharm. Pharm. Sci.* **2014**, *3*, 2214–2228.

(17) Teixeira, P. C.; Leite, G. M.; Domingues, R. J.; Paul, J. S.; Gibbs, A.; Ferreira, J. P. Antimicrobial effects of a microemulsion and a nanoemulsion on enteric and other pathogens and biofilms. *Int. J. Food Microbiol.* **2007**, *118*, 15–9.

(18) Al-Adham, I.; Al-Nawajeh, A.; Khalil, E.; Collier, P. J. The antimicrobial activity of oil-in-water microemulsions is predicted by their position within the microemulsion stability zone. *Int. Arabic J. Antimicrob. Agents* **2012**, *2*, 1–8.

(19) Hamouda, T.; Myc, A.; Donovan, B.; Shih, A. Y.; Reuter, J. D.; Baker, J. R. A novel surfactant nanoemulsion with a unique non-irritant topical antimicrobial activity against bacteria, enveloped viruses and fungi. *Microbiol. Res.* **2001**, *156*, 1–7.

(20) Huh, A. J.; Kwon, Y. J. “Nanoantibiotics”: a new paradigm for treating infectious diseases using nanomaterials in the antibiotics resistant era. *J. Controlled Release* **2011**, *156*, 128–145.

(21) Lee, V. A.; Karthikeyan, R.; Rawls, H. R.; Amaechi, B. T. Anticariogenic effect of a cetylpyridinium chloride-containing nanoemulsion. *J. Dent.* **2010**, *38*, 742–749.

(22) Karthikeyan, R.; Amaechi, B. T.; Rawls, H. R.; Lee, V. A. Antimicrobial activity of nanoemulsion on cariogenic *Streptococcus mutans*. *Arch. Oral Biol.* **2011**, *56*, 437–445.

(23) Ramalingam, K.; Amaechi, B. T.; Ralph, R. H.; Lee, V. A. Antimicrobial activity of nanoemulsion on cariogenic planktonic and biofilm organisms. *Arch. Oral Biol.* **2012**, *57*, 15–22.

(24) Washington, C. Stability of lipid emulsions for drug delivery. *Adv. Drug Delivery Rev.* **1996**, *20*, 131–145.

(25) Mahajan, H.; Dinger, S. Design and in vitro evaluation of nanoemulsion for nasal delivery of artemether. *Indian. J. Novel Drug Delivery* **2011**, *3*, 272–277.

(26) Stenz, L.; François, P.; Fischer, A.; Huyghe, A.; Tangomo, M.; Hernandez, D.; et al. Impact of oleic acid (cis-9-octadecenoic acid) on bacterial viability and biofilm production in *Staphylococcus aureus*. *FEMS Microbiol. Lett.* **2008**, *287*, 149–155.

(27) Barakat, H. S.; Kassem, M. A.; El-Khordagui, L. K.; Khalafallah, N. M. Vancomycin-eluting niosomes: a new approach to the inhibition of staphylococcal biofilm on abiotic surfaces. *AAPS PharmSciTech* **2014**, *15*, 1263–1274.

(28) Shafiq, S.; Shakeel, F.; Talegaonkar, S.; Ahmad, F. J.; Khar, R. K.; Ali, M. Development and bioavailability assessment of ramipril

nanoemulsion formulation. *Eur. J. Pharm. Biopharm.* **2007**, *66*, 227–243.

(29) Kashef, M. T.; Saleh, N. M.; Assar, N. H.; Ramadan, M. A. The Antimicrobial Activity of Ciprofloxacin-Loaded Niosomes against Ciprofloxacin-Resistant and Biofilm-Forming *Staphylococcus aureus*. *Infect. Drug Resist.* **2020**, *13*, 1619–1629.

(30) Hemmila, M. R.; Mattar, A.; Taddonio, M. A.; Arbabi, S.; Hamouda, T.; Ward, P. A.; et al. Topical nanoemulsion therapy reduces bacterial wound infection and inflammation after burn injury. *Surgery* **2010**, *148*, 499–509.

(31) Slomberg, D. L.; Lu, Y.; Broadnax, A. D.; Hunter, R. A.; Carpenter, A. W.; Schoenfisch, M. H. Role of size and shape on biofilm eradication for nitric oxide-releasing silica nanoparticles. *ACS Appl. Mater. Interfaces* **2013**, *5*, 9322–9329.

(32) Bali, V.; Ali, M.; Ali, J. study of surfactant combinations and development of a novel nanoemulsion for minimizing variations in bioavailability of ezetimibe. *Colloids Surf., B* **2010**, *76*, 410–420.

(33) Miastkowska, M.; Sliwa, P. Influence of terpene type on the release from an O/W nanoemulsion: Experimental and theoretical studies. *Molecules* **2020**, *25*, No. 2747.

(34) Kalam, M. A.; Humayun, M.; Parvez, N.; Yadav, S.; Garg, A.; Amin, S.; et al. Release kinetics of modified pharmaceutical dosage forms: a review. *Cont. J. Pharm. Sci.* **2007**, *1*, 30–35.

(35) Azeem, A.; Rizwan, M.; Ahmad, F. J.; Iqbal, Z.; Khar, R. K.; Aqil, M.; Talegaonkar, S. Nanoemulsion components screening and selection: a technical note. *Aaps Pharmscitech* **2009**, *10*, 69–76.

(36) Kumar, H.; Kumar, V. Ultrasonication assisted formation and stability of water-in-oil nanoemulsions: Optimization and ternary diagram analysis. *Ultrason. Sonochem.* **2018**, *49*, 79–88.

(37) Arianto, A.; Cindy, C. Preparation and evaluation of sunflower oil nanoemulsion as a sunscreen. *Open Access Maced. J. Med. Sci.* **2019**, *7*, 3757–3761.

(38) Feng, J.; Chen, W.; Liu, Q.; Chen, Z.; Yang, J.; Yang, W. Development of abamectin-loaded nanoemulsion and its insecticidal activity and cytotoxicity. *Pest Manage. Sci.* **2020**, *76*, 4192–4201.

(39) Duggan, J. M.; Sedgley, C. M. Biofilm formation of oral and endodontic *Enterococcus faecalis*. *J. Endod.* **2007**, *33*, 815–818.